antigen delivery with either BLs or US exposure. In these treated cells, antigen was mainly taken up via the endocytosis pathway. Although we have not confirmed MHC class II presentation, the antigen would presumably be presented on MHC class II molecules to DCs via the general antigen processing mechanism [10]. The exogenous antigens directly delivered into the cytosol would be processed similarly endogenously derived antigens, which are enzymatically digested into peptides, mainly by cytosolic proteases called proteasomes, and are then transported by transporters associated with antigen processing (TAP) molecules into the endoplasmic reticulum (ER). In the ER lumen, peptides bind to MHC class I molecules, which are subsequently transported via the Golgi apparatus to the cell surface [46]. Moreover, immunization of DCs treated with OVA, BLs and US exposure could prime OVA-specific CTLs. This result indicates that DCs presented with OVA-derived epitope peptides on MHC class I molecules effectively prime OVA-specific CTLs *in vivo*. We suspected that the effective priming of antigen-specific CTLs would result in the rejection of tumor cells. As shown in Fig. 5(a), all the immunized mice completely rejected the inoculated tumor cells. Tumor cells were intradermally re-injected into these mice to re-challenge their immune system and assess the preventive effects of immunization for suppressing tumor regeneration (Fig. 5(c)). Rejection following re-challenge with tumor cells suggests the induction of an antigen memory system in the host's immune system, i.e., memory T cells for the immunization antigen. Thus, this therapeutic method has potential for suppressing the regeneration and metastasis of tumors. Finally, we also assessed the therapeutic effects of this treatment towards established tumors (Fig. 6). Immunization with DCs treated with antigen, BLs and US exposure lead to significant therapeutic effects towards established tumors. Tumor cells generally secrete cytokines such as TGF-β to suppress the host's immune system. It is therefore possible that antigen delivery with BLs and US exposure could effectively induce an anti-tumor immune response even in the presence of established tumors.

In conclusion, we have developed a novel system for delivering antigens into DCs using BLs and sonoporation. Immunization of DCs using this antigen delivery system could effectively prime the anti-tumor immune system due to the induction of MHC class I TAA presentation. Therefore, BLs in conjunction with sonoporation might be a useful antigen delivery system for DC-based cancer immunotherapy. In the future, this system will be applied to various antigens containing unknown TAAs, such as crude antigens separated from surgically-removed human tumors.

## Acknowledgments

The authors thank Mr. Shota Otake, Mr. Norihito Nishiie, Mr. Ken Osawa, Ms. Risa Koshima, Ms. Motoka Kawamura, Mr. Ryo Tanakadate, Mr. Kunihiko Matsuo and Mr. Yasuyuki Shiono (Teikyo University) for their technical assistance, and Mr. Yasuhiko Hayakawa, Mr. Takahiro Yamauchi and Mr. Kosho Suzuki (Nepa Gene Co., Ltd.) for their technical advice regarding US exposure. This study was supported by the Program for Promotion of Fundamental Studies in Health Sciences of the National Institute of Biomedical Innovation (NIBIO). Tetsuya Kodama acknowledges the Grant for Research on Nanotechnical Medical, the Ministry of Health, Labour and Welfare of Japan (H19-nano-010).

## References

[1] F.O. Nestle, A. Farkas, C. Conrad, Dendritic-cell-based therapeutic vaccination against cancer, Curr. Opin. Immunol. 17 (2005) 163–169.
[2] J. Copier, A. Dalgleish, Overview of tumor cell-based vaccines, Int. Rev. Immunol. 25 (2006) 297–319.
[3] R.N. Germain, MHC-dependent antigen processing and peptide presentation: providing ligands for T lymphocyte activation, Cell 76 (1994) 287–299.
[4] P. Elamanchili, M. Diwan, M. Cao, J. Samuel, Characterization of poly(D,L-lactic-co-glycolic acid) based nanoparticulate system for enhanced delivery of antigens to dendritic cells, Vaccine 22 (2004) 2406–2412.
[5] T. Yoshikawa, N. Okada, A. Oda, K. Matsuo, K. Matsuo, Y. Mukai, Y. Yoshioka, T. Akagi, M. Akashi, S. Nakagawa, Development of amphiphilic gamma-PGA-nanoparticle based tumor vaccine: potential of the nanoparticulate cytosolic protein delivery carrier, Biochem. Biophys. Res. Commun. 366 (2008) 408–413.
[6] P. Machy, K. Serre, L. Leserman, Class I-restricted presentation of exogenous antigen acquired by Fcgamma receptor-mediated endocytosis is regulated in dendritic cells, Eur. J. Immunol. 30 (2000) 848–857.
[7] N. Okada, T. Saito, K. Mori, Y. Masunaga, Y. Fujii, J. Fujita, K. Fujimoto, T. Nakanishi, K. Tanaka, S. Nakagawa, T. Mayumi, T. Fujita, A. Yamamoto, Effects of lipofectin-antigen complexes on major histocompatibility complex class I-restricted antigen presentation pathway in murine dendritic cells and on dendritic cell maturation, Biochim. Biophys. Acta 1527 (2001) 97–101.
[8] L. Wang, H. Ikeda, Y. Ikuta, M. Schmitt, Y. Miyahara, Y. Takahashi, X. Gu, Y. Nagata, Y. Sasaki, K. Akiyoshi, J. Sunamoto, H. Nakamura, K. Kuribayashi, H. Shiku, Bone marrow-derived dendritic cells incorporate and process hydrophobized polysaccharide/oncoprotein complex as antigen presenting cells, Int. J. Oncol. 14 (1999) 695–701.
[9] K. Kawamura, N. Kadowaki, R. Suzuki, S. Udagawa, S. Kasaoka, N. Utoguchi, T. Kitawaki, N. Sugimoto, N. Okada, K. Maruyama, T. Uchiyama, Dendritic cells that endocytosed antigen-containing IgG-liposomes elicit effective antitumor immunity, J. Immunother. 29 (2006) 165–174.
[10] K.W. Kim, S.H. Kim, J.H. Jang, E.Y. Lee, S.W. Park, J.H. Um, Y.J. Lee, C.H. Lee, S. Yoon, S.Y. Seo, M.H. Jeong, S.T. Lee, B.S. Chung, C.D. Kang, Dendritic cells loaded with exogenous antigen by electroporation can enhance MHC class I-mediated antitumor immunity, Cancer Immunol. Immunother. 53 (2004) 315–322.
[11] J.M. Weiss, C. Allen, R. Shivakumar, S. Feller, L.H. Li, L.N. Liu, Efficient responses in a murine renal tumor model by electroloading dendritic cells with whole-tumor lysate, J. Immunother. 28 (2005) 542–550.
[12] M. Fechheimer, J.F. Boylan, S. Parker, J.E. Sisken, G.L. Patel, S.G. Zimmer, Transfection of mammalian cells with plasmid DNA by scrape loading and sonication loading, Proc. Natl. Acad. Sci. U. S. A. 84 (1987) 8463–8467.
[13] M.W. Miller, D.L. Miller, A.A. Brayman, A review of in vitro bioeffects of inertial ultrasonic cavitation from a mechanistic perspective, Ultrasound Med. Biol. 22 (1996) 1131–1154.
[14] M. Joersbo, J. Brunstedt, Protein synthesis stimulated in sonicated sugar beet cells and protoplasts, Ultrasound Med. Biol. 16 (1990) 719–724.
[15] D.L. Miller, S.V. Pislaru, J.E. Greenleaf, Sonoporation: mechanical DNA delivery by ultrasonic cavitation, Somat. Cell Mol. Genet. 27 (2002) 115–134.
[16] H.R. Guzman, A.J. McNamara, D.X. Nguyen, M.R. Prausnitz, Bioeffects caused by changes in acoustic cavitation bubble density and cell concentration: a unified explanation based on cell-to-bubble ratio and blast radius, Ultrasound Med. Biol. 29 (2003) 1211–1222.
[17] W. Wei, B. Zheng-zhong, W. Yong-jie, Z. Qing-wu, M. Ya-lin, Bioeffects of low-frequency ultrasonic gene delivery and safety on cell membrane permeability control, J. Ultrasound Med. 23 (2004) 1569–1582.
[18] H.J. Kim, J.F. Greenleaf, R.R. Kinnick, J.T. Bronk, M.E. Bolander, Ultrasound-mediated transfection of mammalian cells, Hum. Gene Ther. 7 (1996) 1339–1346.
[19] D.B. Tata, F. Dunn, D.J. Tindall, Selective clinical ultrasound signals mediate differential gene transfer and expression in two human prostate cancer cell lines: LnCap and PC-3, Biochem. Biophys. Res. Commun. 234 (1997) 64–67.
[20] M. Duvshani-Eshet, M. Machluf, Therapeutic ultrasound optimization for gene delivery: a key factor achieving nuclear DNA localization, J. Control. Release 108 (2005) 513–528.
[21] W.J. Greenleaf, M.E. Bolander, G. Sarkar, M.B. Goldring, J.F. Greenleaf, Artificial cavitation nuclei significantly enhance acoustically induced cell transfection, Ultrasound Med. Biol. 24 (1998) 587–595.
[22] Y. Taniyama, K. Tachibana, K. Hiraoka, M. Aoki, S. Yamamoto, K. Matsumoto, T. Nakamura, T. Ogihara, Y. Kaneda, R. Morishita, Development of safe and efficient novel nonviral gene transfer using ultrasound: enhancement of transfection efficiency of naked plasmid DNA in skeletal muscle, Gene Ther. 9 (2002) 372–380.
[23] S. Chen, J.H. Ding, R. Bekeredjian, B.Z. Yang, R.V. Shohet, S.A. Johnston, H.E. Hohmeier, C.B. Newgard, P.A. Grayburn, Efficient gene delivery to pancreatic islets with ultrasonic microbubble destruction technology, Proc. Natl. Acad. Sci. U. S. A. 103 (2006) 8469–8474.
[24] A. Aoi, Y. Watanabe, S. Mori, M. Takahashi, G. Vassaux, T. Kodama, Herpes simplex virus thymidine kinase-mediated suicide gene therapy using nano/microbubbles and ultrasound, Ultrasound Med. Biol. 34 (2008) 425–434.
[25] Z.P. Shen, A.A. Brayman, L. Chen, C.H. Miao, Ultrasound with microbubbles enhances gene expression of plasmid DNA in the liver via intraportal delivery, Gene Ther. (2008).
[26] S. Sonoda, K. Tachibana, E. Uchino, A. Okubo, M. Yamamoto, K. Sakoda, T. Hisatomi, K.H. Sonoda, Y. Negishi, Y. Izumi, S. Takao, T. Sakamoto, Gene transfer to corneal epithelium and keratocytes mediated by ultrasound with microbubbles, Investig. Ophthalmol. Vis. Sci. 47 (2006) 558–564.
[27] K. Iwanaga, K. Tominaga, K. Yamamoto, M. Habu, H. Maeda, S. Akifusa, T. Tsujisawa, T. Okinaga, J. Fukuda, T. Nishihara, Local delivery system of cytotoxic agents to tumors by focused sonoporation, Cancer Gene Ther. 14 (2007) 354–363.
[28] R. Bekeredjian, S. Chen, P.A. Grayburn, R.V. Shohet, Augmentation of cardiac protein delivery using ultrasound targeted microbubble destruction, Ultrasound Med. Biol. 31 (2005) 687–691.
[29] R. Bekeredjian, H.F. Kuecherer, R.D. Kroll, H.A. Katus, S.E. Hardt, Ultrasound-targeted microbubble destruction augments protein delivery into testes, Urology 69 (2007) 386–389.
[30] T. Yamashita, S. Sonoda, R. Suzuki, N. Arimura, K. Tachibana, K. Maruyama, T. Sakamoto, A novel bubble liposome and ultrasound-mediated gene transfer to ocular surface: RC-1 cells in vitro and conjunctiva in vivo, Exp. Eye Res. 85 (2007) 741–748.

[31] R. Suzuki, T. Takizawa, Y. Negishi, K. Hagisawa, K. Tanaka, K. Sawamura, N. Utoguchi, T. Nishioka, K. Maruyama, Gene delivery by combination of novel liposomal bubbles with perfluoropropane and ultrasound, J. Control. Release 117 (2007) 130–136.
[32] R. Suzuki, T. Takizawa, Y. Negishi, N. Utoguchi, K. Maruyama, Effective gene delivery with novel liposomal bubbles and ultrasonic destruction technology, Int. J. Pharm. 354 (2008) 49–55.
[33] R. Suzuki, T. Takizawa, Y. Negishi, N. Utoguchi, K. Sawamura, K. Tanaka, E. Namai, Y. Oda, Y. Matsumura, K. Maruyama, Tumor specific ultrasound enhanced gene transfer in vivo with novel liposomal bubbles, J. Control. Release 125 (2008) 137–144.
[34] R. Suzuki, T. Takizawa, Y. Negishi, N. Utoguchi, K. Maruyama, Effective gene delivery with liposomal bubbles and ultrasound as novel non-viral system, J. Drug Target. 15 (2007) 531–537.
[35] J.D. Pfeifer, M.J. Wick, R.L. Roberts, K. Findlay, S.J. Normark, C.V. Harding, Phagocytic processing of bacterial antigens for class I MHC presentation to T cells, Nature 361 (1993) 359–362.
[36] K. Inaba, M. Inaba, M. Deguchi, K. Hagi, R. Yasumizu, S. Ikehara, S. Muramatsu, R.M. Steinman, Granulocytes, macrophages, and dendritic cells arise from a common major histocompatibility complex class II-negative progenitor in mouse bone marrow, Proc. Natl. Acad. Sci. U. S. A. 90 (1993) 3038–3042.
[37] D.P. Guo, X.Y. Li, P. Sun, Y.B. Tang, X.Y. Chen, Q. Chen, L.M. Fan, B. Zang, L.Z. Shao, X.R. Li, Ultrasound-targeted microbubble destruction improves the low density lipoprotein receptor gene expression in HepG2 cells, Biochem. Biophys. Res. Commun. 343 (2006) 470–474.
[38] T. Mosmann, Rapid colorimetric assay for cellular growth and survival: application to proliferation and cytotoxicity assays, J. Immunol. Methods 65 (1983) 55–63.
[39] S.E. Slezak, P.K. Horan, Cell-mediated cytotoxicity. A highly sensitive and informative flow cytometric assay, J. Immunol. Methods 117 (1989) 205–214.
[40] G. Reinhard, A. Marten, S.M. Kiske, F. Feil, T. Bieber, I.G. Schmidt-Wolf, Generation of dendritic cell-based vaccines for cancer therapy, Br. J. Cancer 86 (2002) 1529–1533.
[41] M. Kinoshita, K. Hynynen, Intracellular delivery of Bak BH3 peptide by microbubble-enhanced ultrasound, Pharm. Res. 22 (2005) 716–720.
[42] I.V. Larina, B.M. Evers, R.O. Esenaliev, Optimal drug and gene delivery in cancer cells by ultrasound-induced cavitation, Anticancer Res. 25 (2005) 149–156.
[43] M. Duvshani-Eshet, D. Adam, M. Machluf, The effects of albumin-coated microbubbles in DNA delivery mediated by therapeutic ultrasound, J. Control. Release 112 (2006) 156–166.
[44] C.M. Newman, T. Bettinger, Gene therapy progress and prospects: ultrasound for gene transfer, Gene Ther. 14 (2007) 465–475.
[45] R.K. Schlicher, H. Radhakrishna, T.P. Tolentino, R.P. Apkarian, V. Zarnitsyn, M.R. Prausnitz, Mechanism of intracellular delivery by acoustic cavitation, Ultrasound Med. Biol. 32 (2006) 915–924.
[46] P.M. Kloetzel, Antigen processing by the proteasome, Nat. Rev. Mol. Cell. Biol. 2 (2001) 179–187.

Tohoku J. Exp. Med., 2010, **220**, 199-206

# Evaluating the Role of Rheumatoid Factors for the Development of Rheumatoid Arthritis in a Mouse Model with a Newly Established ELISA System

**Yuki Tanaka,[1,2] Hiroaki Komori,[1*] Shiro Mori,[3] Yoshiko Soga,[1] Takahito Tsubaki,[1] Miho Terada,[1] Tatsuhiko Miyazaki,[1] Takahiro Fujino,[2] Satoshi Nakamura,[4] Hiroyuki Kanno,[5] Tatsuya Sawasaki,[6] Yaeta Endo[6] and Masato Nose[1,7]**

[1]Department of Pathogenomics, Ehime University Graduate School of Medicine, Ehime, Japan
[2]Integrated Center for Sciences, Ehime University, Ehime, Japan
[3]Department of Oral and Maxillofacial Surgery, Tohoku University Graduate School of Dentistry, Sendai, Japan
[4]Department of Bioengineering, Tokyo Institute of Technology, Tokyo, Japan
[5]Department of Pathology, Iwate University School of Medicine, Morioka, Japan
[6]Cell-Free Science and Technology Research Center, Ehime University, Ehime, Japan
[7]Proteo-Medicine Research Center, Ehime University, Ehime, Japan

Enzyme-linked immunosorbent assays (ELISA) have been widely used to determine quantitatively autoantibodies. However, the processes for the purification and immobilization of antigens in conventional ELISA methods include multiple steps, which have hampered the application for screening of autoantibodies. Here, we have developed a novel ELISA system using the plates pre-coated with glutathione casein to capture recombinant proteins fused to N-terminal glutathione S-transferase (GST). The GST-fused proteins were synthesized with the wheat germ cell-free protein production system. Thus, the present system combined the GST-capture ELISA with the cell-free protein production system, which allowed immobilization of the recombinant proteins with one-step purification. Using this ELISA method, we determined whether rheumatoid factors (RF), which have been considered as one of the representative disease – specific autoantibodies for rheumatoid arthritis (RA), were genetically associated with severity of arthritis in a mouse model for RA, MRL/Mp-*lpr/lpr* (MRL/lpr). GST-fused human IgG1-Fc (GST-Fc), synthesized with the robotic protein synthesizer, were used as reactants for RF. Serum samples for RF were prepared from 11 lines of a recombinant inbred mouse strain, MXH/lpr, which was established from intercrosses between MRL/lpr and non-arthritic C3H/HeJ-*lpr/lpr* (C3H/lpr) strains, composed of a different genomic recombination derived from the parental strains in each line. A correlation of RF titers with the severity of the arthritis in these lines was not significant, indicating genetic dissociation of RF from arthritis and that RF is not necessarily required for the development of RA. The present method may provide high-throughput screening for determining the disease-specific autoantibodies in autoimmune diseases.

**Keywords:** MRL/lpr; recombinant inbred strain; MXH/lpr; GST; IgG-Fc
Tohoku J. Exp. Med., 2010, **220** (3), 199-206. 

Enzyme-linked immunosorbent assays (ELISA) have been widely used to determine quantitatively the reactant proteins for autoantibodies in various diseases involving autoimmunity and infection (Gawryl et al. 1986; Moore et al. 1986; Tan 1989; Valdés Veliz et al. 2003). However, conventional ELISA methods are not suitable for the wide screening of autoantibodies because various processes and conditions are necessary for the purification and immobilization of each protein.

The wheat germ cell-free protein production system was established in our laboratory, in which any proteins could be synthesized in the presence of the cDNA template by using wheat germ ribosome more effectively than in *E. coli*-based system (Madin et al. 2000; Sawasaki et al. 2002a), and made it possible to synthesize proteins in a high-throughput manner (Sawasaki et al. 2002b). In fact, almost 380 kinds of proteins could be automatically synthesized at once overnight based on cDNA templates by using the robotic protein synthesizer GenDecorder 1000A® (CellFree Sciences, Matsuyama, Japan). Among cell-free

Received October 14, 2009; revision accepted for publication January 20, 2010. doi:10.1620/tjem.220.199
*Deceased March 7, 2009
Correspondence: Masato Nose, M.D., Ph.D., Department of Pathogenomics, Ehime University Graduate School of Medicine, Shitsukawa, Toon, Ehime 791-0295, Japan.
e-mail; masanose@m.ehime-u.ac.jp

systems for protein synthesis, this wheat germ-based system is of special interest for its eukaryotic nature; it has the significant advantage of producing a large amount of eukaryotic multi-domain proteins in folded state (Endo and Sawasaki 2006; Goshima et al. 2008; Takai et al. 2010). Thus, this system may be suitable for high-throughput synthesis of any reactant proteins for autoantibodies. Moreover, when recombinant proteins fused to N-terminal glutathione S-transferase (GST) are prepared in this system and captured on glutathione-coated ELISA plates (Sehr et al. 2001), the multi-step processes for the purification and immobilization of each protein required in conventional ELISA methods may not be necessary.

This report describes the development of a capture ELISA system using synthesized proteins fused to GST in the wheat germ cell-free protein production system. This method allowed the simple immobilization and purification of the proteins in one-step on ELISA plates pre-coated with glutathione casein. Then, this system was used to measure the rheumatoid factor (RF) in a murine model for rheumatoid arthritis (RA), MRL/Mp-*lpr/lpr* (MRL/lpr) (Murphy and Roths 1978; Nose et al. 1989). This mouse strain spontaneously develops arthritis resembling RA associated with high titers of IgG-RF, supporting the concept that IgG RF is one of disease-specific autoantibodies in RA (Theofilopoulos and Dixon 1985). Our results may reveal that the RF activity does not genetically correlate with the severity of arthritis in this model.

## Materials and Methods

*IgG-Fc with GSTtag in cell free system*

The Fc portion of human IgG1 (IgG-Fc) was prepared as RF reactant according to a cell-free protein synthesis system using wheat germ ribosomal RNA (Madin et al. 2000; Sawasaki et al. 2002a; Soga et al. 2009). In brief, the Fc portion of human IgG1 cDNA (Kitai et al. 1988) was inserted into a pEUE01-GST-N2 expression vector (CellFree Sciences, Matsuyama, Japan) containing a GST region and SP6 promotor. The GST-IgG-Fc proteins were automatically synthesized by the Robotic Protein Synthesizer Protemist® DT (CellFree Sciences) as previously described (Soga et al. 2009). Namely, 250 $\mu$l of transcription mixture containing 25 $\mu$g of the plasmid DNA, 80 mM HEPES-potassium hydroxide, pH 7.8, 16 mM magnesium acetate, 2 mM spermidine, 10 mM dithiothreitol, 2.5 mM each of nucleoside triphosphates, 250 U of SP6 RNA polymerase (Promega, Madison, WI, USA) and 250 U of RNasin (Promega) was incubated for 6 hr at 37°C. After the incubation, the transcription solution containing transcribed mRNA was mixed with 250 $\mu$l of wheat germ extract WEPRO1240 (CellFree Sciences) supplemented with 2 ml of 20 mg/ml creatine kinase in a single well of a six-well plate. The 5.5 ml substrate mix (30 mM HEPES-potassium hydroxide, pH 7.8, 100 mM potassium acetate, 2.7 mM magnesium acetate, 0.4 mM spermidine, 2.5 mM dithiothreitol, 0.3 mM amino acid mix, 1.2 mM ATP, 0.25 mM GTP and 16 mM creatine phosphate; CellFree Sciences) was then added on top of the translation mix and then was incubated at 17°C for 20 hr. The reaction mixture was used without any purification procedures as IgG-Fc-GST to be captured on the ELISA plates. In some experiments, the IgG-Fc-GST in the mixture was purified by glutathione Sepharose 4B (GE Healthcare, Uppsala, Sweden) according to the instructions for use.

*GST capture ELISA*

GST capture ELISA was performed basically according to the previously described method (Sehr et al. 2001). In brief, to conjugate glutathione to casein, casein (Wako, Osaka, Japan) at a concentration of 5 mg/ml in phosphate-buffered saline (PBS) was incubated at room temperature (RT) with 0.4 mM N-ethylmaleimide (NEM; Sigma-Aldrich, St. Louis, MO, USA) and then the single cysteine residue was blocked in casein. Next, sulfosuccinimidyl 4-[p-maleimidophenyl] butyrate (SSMBP; Pierce, Rockford, IL) was added at 4 mM as a cross-linker. Free SSMBP and NEM were separated from casein on PD10 columns (GE Healthcare). The protein fraction was then supplemented with 10 mM glutathione (Wako) and the coupling reaction was executed for 1 h at RT. The glutathione casein was separated from unbound glutathione by gel filtration with PD10, using PBS as buffer and stored at –20°C until use. Next, plastic plates, consisting of 96 wells (Thermo Labsystems, Franklin, MA), were coated overnight at 4°C with 100 $\mu$l/well of glutathione casein, 2 $\mu$g/ml in 50 mM carbonate buffer, pH 9.6. The optimal concentration of glutathione casein was determined in a titration study by using plates pre-coated with it in a various concentration (0.5 to 8 $\mu$g/ml). Thereafter, the wells were incubated for 1 h at 37°C with blocking buffer (0.2% casein in PBS, 0.05% Tween 20), followed by incubation for 1 h at 4°C with the reaction mixture (100 $\mu$l/well) of IgG-Fc-GST proteins synthesized in cell free system diluted in blocking buffer.

The coated ELISA plates were then incubated for 1 h with 100 $\mu$l/well of goat anti-human IgG-Fc antibodies conjugated with alkaline phosphatase (AP; Sigma-Aldrich) or diluted sample solution of mouse monoclonal antibodies and mouse sera. Bound antibodies of the later were detected by polyclonal goat anti-mouse immunoglobulin IgG (Sigma) or IgM (Zymed Laboratories Inc., San Francisco, CA), conjugated to AP, diluted 1/2000 in blocking buffer. In some experiments, the conventional ELISA using *E. coli.*-generated IgG-Fc with the same construct (Nose et al. 1990) which were purified by protein A column (GE Healthcare) was performed in the same procedure. Commercialized glutathione-coated ELISA plates for GST-proteins, which are pre-coupled with glutathione via polyethylene glycol as a spacer, were reacted overnight at 4°C with GST or IgG-Fc-GST proteins synthesized in cell free system according to the manufacturer instructions.

*Mouse sera*

Serum samples for RF were prepared from MRL/MpJ-*lpr/lpr* (MRL/lpr) and C3H/HeJ-*lpr/lpr* (C3H/lpr) mice and 11 lines of a recombinant inbred (RI) strain of mice, MXH/lpr, established by intercrosses between an MRL/lpr and a C3H/lpr strain of mice. These lines had a different genome recombination each other derived from the parental strains in homozygote. Sera from C3H/HeJ mice without the *lpr* gene were used as normal control for RF. The parental strains of mice were originally obtained from Jackson Laboratory (Bar Harbor, ME). All of the mice used in this study were bred and housed in an animal facility in a pathogen-free and climate-controlled environment with 12 hr light/dark cycles. All experiments were done according to the Guidelines for the Care and Use of Laboratory Animals at Ehime University.

*RF monoclonal antibodies*

Hybridomas producing IgM-RF monoclonal antibodies (clones; Zao2 and Zao7) were prepared by the cell fusion of NS-1 myeloma cells with unmanipulated spleen cells from a 20 wk-old male C57BL/6-*lpr/lpr* mouse, which were originally obtained from the Jackson Laboratory (Bar Harbor), according to a method described elsewhere (Takahashi et al. 1993). The selection of IgM-RF-producing hybridoma cells was performed in conventional ELISA using *E. coli.*-generated IgG-Fc (Nose et al. 1996). Ant-TNP monoclonal IgM antibodies (a mouse hybridoma clone; Sp6) (Nose and Wigzell 1983) were used as a murine IgM control.

*Histopathology of arthritis*

The mice were killed under ether anesthesia, and their hind limbs were processed for histopathology. Whole ankle joints were fixed in 10% formalin in 0.001 M phosphate buffer, pH 7.2, decalcified in 10% formic acid, and embedded in paraffin. Serial sections 2-3-$\mu$m thick were taken sagittally through the talus and stained with hematoxylin and eosin for examinations by light microscopy. The lesions, including the calcaneus bone and anterior and posterior synovial tissue at the ankle joints, were evaluated histopathologically. To evaluate the severity of synovitis, the following grading was used: normal, grade 0; thickening and proliferation of synovial lining, grade 1; and grade 1 with granulomatous and/or fibrous lesions in synovial sublining tissue, grade 2 (Kamogawa et al. 2002). Pannus formation was categorized as follows: normal, grade 0, extending to bone cortex, grade 1; and further to bone marrow, grade 2. Each score of synovitis and pannus formation in the individual mice was represented as the maximum score in the bilateral ankles.

*Statistical analysis*

Student's *t*-test was applied to analyze the statistical significance of the results. A $p$ value of $< 0.05$ was considered to be significant. Correlation between any two parameters of the severity of arthritis and RF activity; synoviti vs. pannus, IgG-RF vs. IgM-RF, IgG-RF vs. synovitis/pannus, and IgM-RF vs. synovitis/pannus, was estimated by the Spearman rank-correlation coefficient as indicated $r$.

## Results

*One-step capture of IgG-Fc-GST fusion proteins on the ELISA plates*

Synthetic IgG-Fc-GST in the reaction mixture was successfully captured on ELISA plates coated with glutathione-conjugated casein. The reaction mixtures of GST or IgG-Fc-GST prepared in cell free system themselves showed multiple bands on PAGE as shown in Fig. 1A. However, each fraction obtained after reacting on and then eluting from the ELISA plates coated with glutathione-conjugated casein, but not with casein only, clearly showed a single band with the expected molecular sizes corresponding GST or GST-IgG-Fc, except a few extra bands with 22-25kD in molecular sizes derived from wheat germ extract (Fig. 1B).

The dose dependency of IgG-Fc capture on the glutathione casein-coated plates was measured by using anti-human IgG-Fc antibodies (Fig. 2). Synthetic IgG-Fc-GST in the reaction mixture was reacted with the glutathione casein-coated plates at a series of concentrations generated by serial dilution. The results showed the capture of IgG-Fc-GST to be saturated at concentrations of less than 1.0 $\mu$g/ml under this condition. The background coating only with glutathione casein was quite low and GST itself did not react at any concentrations.

*Reactivity of monoclonal RF on the capture ELISA*

Next, to confirm the specificity of RF reactivity of the

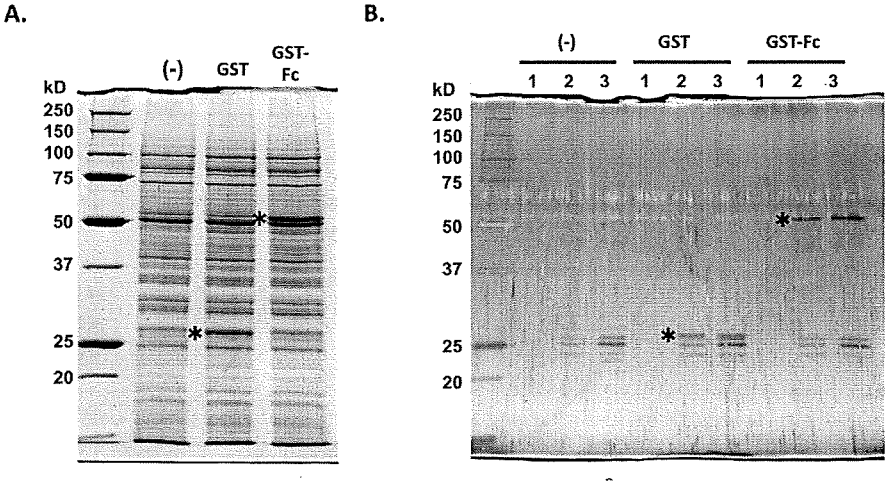


Fig. 1. Capture of the synthetic IgG-Fc-GST on glutathione casein-coated ELISA plates. A. The reaction mixture (0.5 $\mu$l) of vector free (–), GST or IgG-Fc-GST was loaded on SDS-PAGE. B. The same mixture of samples (100 $\mu$l) was loaded after reacting on and then eluting by using 10 $\mu$l of elution buffer (50 mM Tris-HCl, 10 mM reduced glutathione, pH8.0) from the ELISA plates coated with; casein only (lane 1) or glutathione-conjugated casein (10 mg/ml; lane 2, 1 mg/ml; lane 3). Each eluate (0.5 $\mu$l) was loaded on SDS-PAGE. GST and IgG-Fc-GST seemed to be specifically bound to the glutathione casein-coated plates. Extra bands around 25 kDa seemed to be from wheat germ extract. Asterisk indicates the expected band on each lane.

capture ELISA plates, the reactivity of mouse monoclonal IgM RF, clones Zao2, Zao7 and Sp6 (see Materials and Methods) was compared with that of the conventional ELISA plates coated with *E. coli.*-generated IgG-Fc (Fig. 3). Both monoclonal IgM RF showed almost the same reactivity between the capture ELISA and the conventional ELISA systems. And, mouse IgM control showed no reactivity in both ELISA systems.

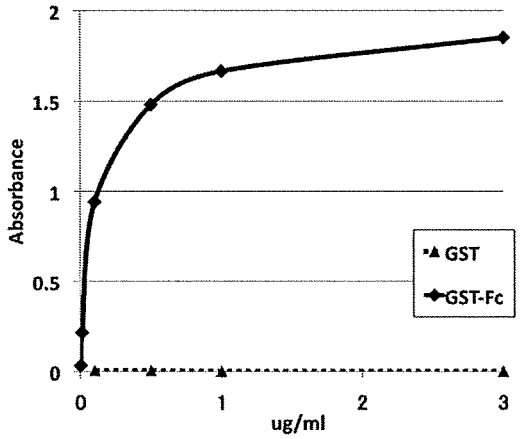


Fig. 2. Dose dependency of IgG-Fc to be captured on the glutathione casein-coated plates. IgG-Fc-GST in the reaction mixture was loaded on the glutathione casein coated plates. The binding of IgG-Fc-GST was measured by using AP-conjugated anti-human IgG-Fc antibodies. The capture of IgG-Fc-GST was in dose-dependent manner, and saturated at concentrations of less than 1.0 $\mu$g/ml. The coating background with glutathione casein was quite low and GST itself did not react at any concentration. Absorbance indicates the mean value of $OD_{405}$-$OD_{510}$ in triplicate samples.

*Measurement of RF activity of mouse sera*

Finally, the IgG RF activity in mouse sera was compared between the arthritis-prone strain of mice MRL/lpr and the non-arthritic strain of mice C3H/lpr, both of which possess the Fas deletion mutant lpr (Nagata, 1994) (Fig. 4A). MRL/lpr mice showed a higher reactivity than C3H/lpr mice as previously reported (Theophilopoulus and Dixon 1985). And, sera from C3H/HeJ mice without the *lpr* gene showed no reactivity for IgG-Fc. At the same time, the results were compared with those obtained using commercialized GST-ELISA plates (Fig. 4B). Unexpectedly, GST-ELISA did not show any IgG-Fc specificity in both mouse sera.

*Genetic dissociation of RF activity from the severity of arthritis in the MXH/lpr mice*

The capture ELISA system was used to determine the correlations between the RF activity and the severity of arthritis in the recombinant inbred strains of mice, MXH/lpr. MXH/lpr mice were established by intercrosses between MRL/lpr and C3H/lpr strains of mice, among which genetic dissociation of arthritis might be generated due to genome recombination between the parental stains, based on a previous study of chromosomal mapping of the susceptibility loci to arthritis (Nose et al. 1989; Kamogawa et al. 2002). Expectedly, genetic dissociation of arthritis was observed among the MXH/lpr mice (Fig. 5); that is, several lines among the MXH/lpr mice showed a significantly higher score in the severity of synovitis (lines; 07, 10, 25 and 36) ($p < 0.05$ vs. C3H/lpr) and pannus formation (lines; 10, 25 and 36) ($p < 0.05$ vs. C3H/lpr) while others such as lines 51

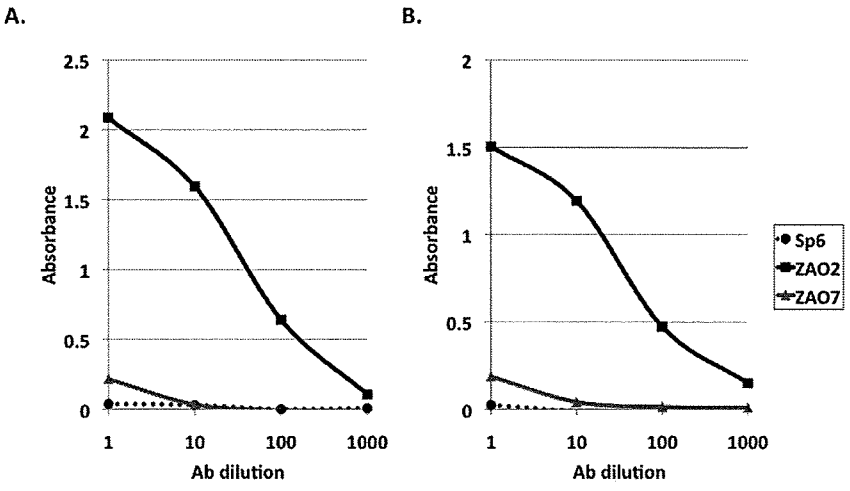


Fig. 3. Reactivity of monoclonal RF on the capture ELISA and the conventional ELISA systems. The culture supernatant of the hybridomas producing IgM monoclonal RF (clones; Zao2 and Zao7) and IgM monoclonal anti-TNP antibodies (clone; Sp6) was reacted on the capture ELISA (A) and the conventional ELISA (B) systems in a serial dilution. These antibodies showed almost the same reactivity between both ELISA systems. Absorbance indicates the mean value of $OD_{405}$-$OD_{510}$ in triplicate samples.

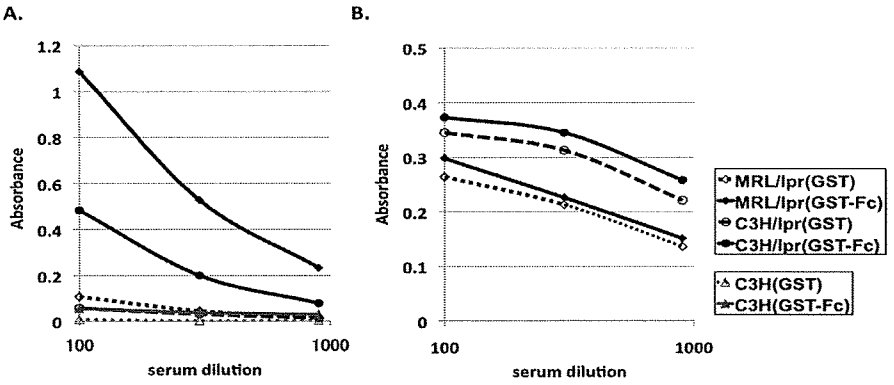


Fig. 4. RF activity of the mouse sera. The mouse sera from male mice of an arthritis-prone stain of mice, MRL/lpr and non-arthritic strain of mice, C3H/lpr (pooled sera at 16-20 weeks old, $n = 5$ each) were compared in a serial dilution. A. The capture ELISA plates, showed the sera from MRL/lpr mice was greater than those from C3H/lpr mice. The normal control sera from C3H/HeJ mice (pooled sera at 8 weeks old, $n = 12$) showed no reactivity. B. The same samples were measured on commercialized GST-ELISA plates. The results showed higher background, thus indicating the reaction to be non-specific for IgG-Fc. Absorbance indicates the mean value of $OD_{405}$-$OD_{510}$ in triplicate samples.

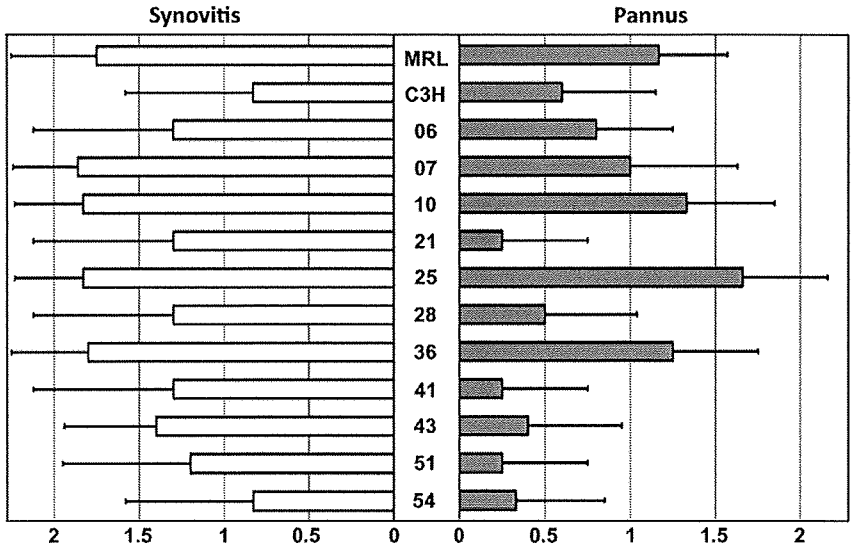


Fig. 5. Genetic dissociation of arthritis among the recombinant inbred strains MXH/lpr. The severity of arthritis of individual mice was graded at 16-20 weeks old ($n = 4$-6 each) and the results were represented as the average total score +/− S.D. of each strain (see Materials and Methods).

and 54 showed a lower score in the both severity. In addition, the severity between synovitis and pannus formation was highly correlated ($r = 0.725$, Fig. 7A), indicating that both lesions are on the same pathological sequence leading arthritis.

Then, the IgM- and IgG-RF activity of each stain of MXH/lpr mice was measured. As shown in Fig. 6, it was clearly demonstrated that IgM- and IgG-RF activity was also genetically dissociated among the MXH/lpr mice. IgG-RF activity of the line 41 was extremely higher than even the arthritis-prone parental strain of mice MRL/lpr ($p < 0.01$) and IgM-RF activity of the lines 06 and 36 was also higher than that of both parental strains ($p < 0.01$). There was only a slight negative correlation between both activities ($r = -0.286$, Fig. 7B).

Finally, correlation between the severity of arthritis and RF activity was examined. There was only a slight positive correlation between any two parameters; IgM-RF or IgG-RF vs. synovitis or pannus formation ($r < 0.265$ in any combinations, Fig. 7C and D).

## Discussion

This study presented a novel method combining the GST-capture ELISA and the wheat germ cell-free protein

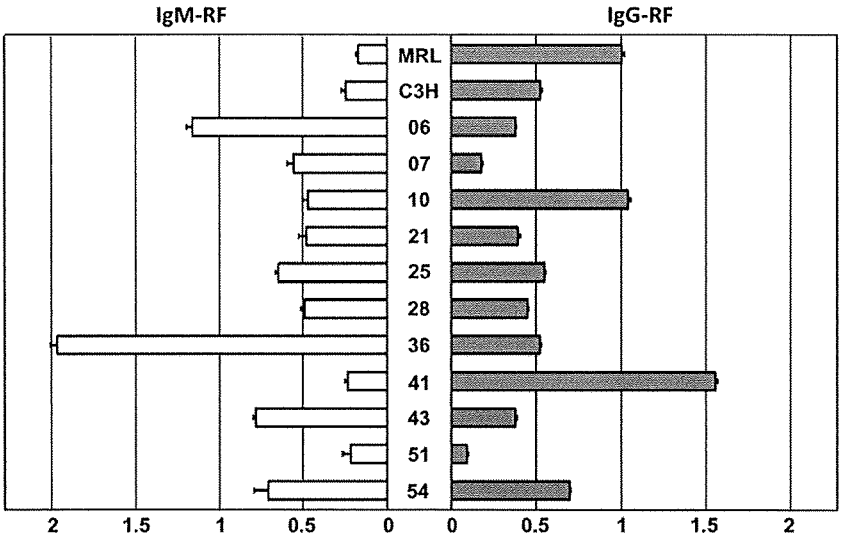


Fig. 6. Genetic dissociation of the RF activity among the recombinant inbred strains MXH/lpr. Mouse sera from each strain of male MXH/lpr mice were pooled at 16-20 weeks old, and they were reacted on the capture ELISA plates following a 100 × dilution. The results were represented as the average total score +/– S.D. in triplicate samples. Each of the studies was repeated three times and the similar results were obtained in all experiments.

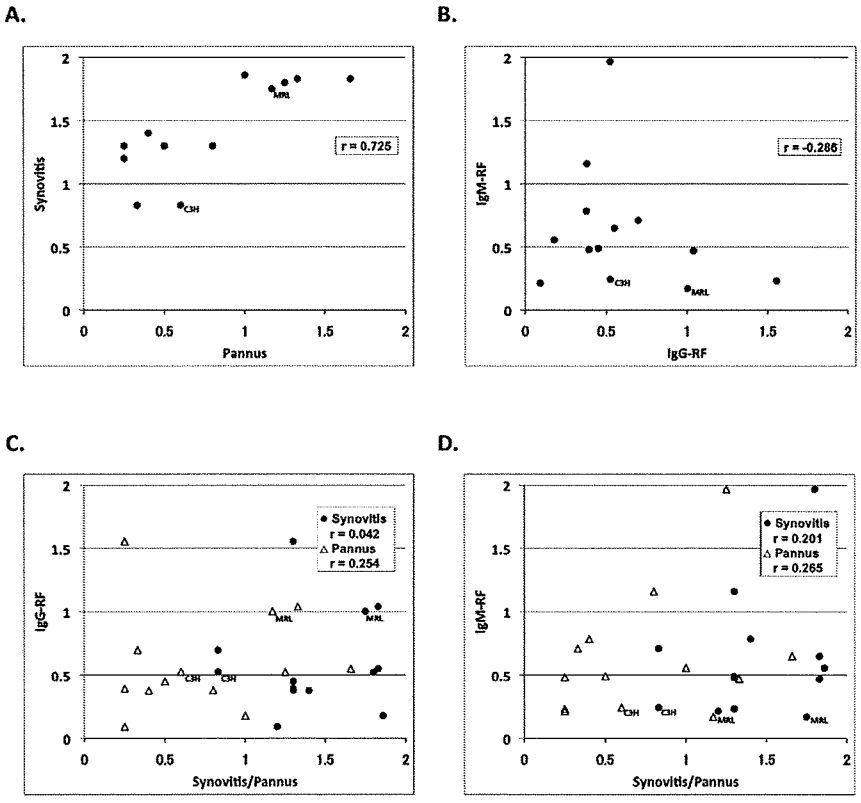


Fig. 7. Correlations of the severity of arthritis and RF activity. A correlation between any two parameters of the severity of arthritis and RF activity was estimated with the Spearman rank-correlation coefficient as indicated by *r*. A; synoviti vs. pannus, B; IgG-RF vs. IgM-RF, C; IgG-RF vs. synovitis/pannus and D; IgM-RF vs. synovitis/pannus.

production system, which thus provides high-throughput screening to clarify disease-specific autoantibodies in autoimmune diseases. The key points of this system are, first, to be able to use any kind of recombinant proteins fused to GST synthesized in the cell-free system without any purification processes, and second, to immobilize them on ELISA plates pre-coated with glutathione casein in one-step and at once.

This system was used to actually measure RF reacting with recombinant IgG-Fc with GST synthesized in the cell-free system. First, the RF specificity of this system was compared with a conventional ELISA containing *E. coli*-generated IgG-Fc using two types of monoclonal IgM-RF with a higher affinity and lower affinity. The results were similar between the two systems (Fig. 3). Next, the IgG-RF activity in mouse sera derived from MRL/lpr and C3H/lpr mice, which has higher RF activity in the former and lower in the later (Theofilopoulos and Dixon 1985), was measured, and compared their specificity with commercialized glutathione-coated ELISA plates. The results showed that the commercialized ELISA showed not only increased background but also absence of specific reactivity (Fig. 4B).

Then, this method was used to clearly demonstrate the genetic dissociation of RF from arthritis in a mouse model for RA. RI strains of mice MXH/lpr mice were prepared using two different parental inbred strains as progenitors, MRL/lpr and C3H/lpr mice, followed by an F1 intercross and more than 20 generations of strict brother-sister mating. This breeding protocol allows the production of a family of new inbred strains with special properties relative to each other since the genome of each RI strain consists of a random combination of genomes. MXH/lpr mice are the first RI strains in autoimmune disease model mice. In this study, the severity of arthritis was different among the strains, thus indicating that genome recombination between the parental strains regulates the severity of arthritis (Fig. 5). A previous study (Kamogawa et al. 2002) suggested that arthritis in MRL/lpr mice is under the control of multiple gene loci with an allelic combination derived from the original inbred strains by chromosomal mapping of the susceptibility loci to arthritis by using the backcross progeny of MRL/lpr × (MRL/lpr × C3H/lpr) F1 mice. The present results verified this proposed concept more clearly by using RI strains on the ground of the reason as described below.

In general, the genetic analysis of disease phenotypes by crossing disease-prone and non-disease prone strains allows for the examination of only the phenotype of one individual in an association with genotypes. This may make it difficult to analyze complex disease phenotypes in a reproducible fashion (Theofilopoulos et al. 1989). In this respect, a set of inbred strains having a genomic mosaic of progenitor strains such as MXH/lpr is considered to be a highly appropriate tool for analyzing the disease phenotypes in a reproducible fashion. In fact, the current study demonstrated genetic dissociation of the severity of arthritis and the RF activity (Figs. 6 and 7). RF has been considered as the argument that RA is an autoimmune disease, and also as the disease-specific autoantibodies in RA. However, the specificity and sensitivity of RF to RA are still controversial and a pathological basis of RA negative for RF, so called sero-negative RA, remains unclear. Our results may indicate that RF activity is not associated with the development of arthritis at least in this mouse model, and other autoantibodies, if present, could be considered as pathogenic autoantibodies.

Not only arthritis, but also other pathological phenotypes might be genetically segregated from autoantibodies, which have been reported as disease-specific antibodies. Therefore, the system using the capture ELISA with many synthetic proteins in cell free system may thus make it possible to perform a screening study of the protein reactants of autoantibodies and verify their significance for disease phenotypes in mouse models and also humans.

## Acknowledgments

This work was supported by Research Funds from the Ministry of Health and Welfare of Japan and the Grant-in Aid for Scientific Research (B) of the Ministry of Education, Science and Culture of Japan (#18390123).

## References

Endo, Y. & Sawasaki, T. (2006) Cell-free expression systems for eukaryotic protein production. *Curr. Opin. Biotech.*, **17**, 373-380.

Gawryl, M.S., Simon, M.T., Eatman, J.L. & Lint, T.F. (1986) An enzyme-linked immunoabsorbent assay for the quantitation of the terminal complement complex from cell membranes or in activated human sera. *J. Immunol. Methods*, **95**, 217-225.

Goshima, N., Kawamura, Y., Fukumoto, A., Miura, A., Honma, R., Satoh, R., Wakamatsu, A., Yamamoto, J., Kimura, K., Nishikawa, T., Andoh, T., Iida, Y., Ishikawa, K., Ito, E., Kagawa, N., Kaminaga, C., Kanehori, K., Kawakami, B., Kenmochi, K., Kimura, R., Kobayashi, M., Kuroita, T., Kuwayama, H., Maruyama, Y., Matsuo, K., Minami, K., Mitsubori, M., Mori, M., Morishita, R., Murase, A., Nishikawa, A., Nishikawa, S., Okamoto, T., Sakagami, N., Sakamoto, Y., Sasaki, Y., Seki, T., Sono, S., Sugiyama, A., Sumiya, T., Takayama, T., Takayama, Y., Takeda, H., Togashi, T., Yahata, K., Yamada, H., Yanagisawa, Y., Endo, Y., Imamoto, F., Kisu, Y., Tanaka, S., Isogai, T., Imai, J., Watanabe, S. & Nomura, N. (2008) Human protein factory for converting the transcriptome into an in vitro–expressed proteome. *Nat. Methods*, **5**, 1011-1017.

Kamogawa, J., Terada, M., Mizuki, S., Nishihara, M., Yamamoto, H., Mori, S., Abe, Y., Morimoto, K., Nakatsuru, S., Nakamura, Y. & Nose, M. (2002) Arthritis in MRL/lpr mice is under the control of multiple gene loci with an allelic combination derived from the original inbred strains. *Arthritis Rheum.*, **46**, 1067-1074.

Kitai, K., Kudo, T., Nakamura, S., Masegi, T., Ichikawa, Y. & Horikoshi, K. (1988) Extracellular production of human immunoglobulin G Fc region (hIgG-Fc) by *Escherichia coli*. *Appl. Microbiol. Biotechnol.*, **28**, 52-59.

Madin, K., Sawasaki, T., Ogasawara, T. & Endo, Y. (2000) A highly efficient and robust cell-free protein synthesis system prepared from wheat embryos: plants apparently contain a suicide system directed at ribosomes. *Proc. Natl. Acad. Sci. USA*, **97**, 559-564.

Moore, T.L., Dorner, R.W. & Zuckner, J.J. (1986) 19S IgM rheu-

matoid factor-7S IgG rheumatoid factor immune complexes isolated in patients with rheumatoid arthritis. *J. Lab. Clin. Med.*, **107**, 465-470.

Murphy, E.D. & Roths, J.B. (1978) Autoimmunity and lymphoproliferation: induction by mutant gene lpr, and acceleration by a male-associated factor in strain BXSB mice. In Rose, N.R., Bigazzai, P.E. & Warner, N.L., editors. Genetic control of autoimmune disease. *New York: Elsevier North Holland*, 207-220.

Nagata, S. (1994) Fas and Fas ligand: a death factor and its receptor. *Adv. Immunol.*, **57**, 129-144.

Nose, M., Nishimura, M., Ito, M.R., Itoh, J., Shibata, T. & Sugisaki, T. (1996) Arteritis in a novel congenic strain of mice derived from MRL/lpr lupus mice: Genetic dissociation from glomerulonephritis and limited autoantibody production. *Am. J. Pathol.*, **149**, 1763-1769.

Nose, M., Nishimura, M. & Kyogoku, M. (1989) Analysis of granulomatous arteritis in MRL/Mp autoimmune disease mice bearing lymphoproliferative genes. The use of mouse genetics to dissociate the development of arteritis and glomerulonephritis. *Am. J. Pathol.*, **135**, 271-280.

Nose, M., Takano, R., Nakamura, S., Arata, Y. & Kyogoku, M. (1990) Recombinant Fc of human IgG1 prepared in an Escherichia coli system escapes recognition by macrophages. *Int. Immunol.*, **2**, 1109-1112.

Nose, M. & Wigzell, H. (1983) Biological significance of carbohydrate chains on monoclonal antibodies. *Proc. Natl. Acad. Sci. USA*, **80**, 6632-6636.

Sawasaki, T., Hasegawa, Y., Tsuchimochi, M., Kamura, N., Ogasawara, T., Kuroita, T. & Endo, Y. (2002a) A bilayer cell-free protein synthesis system for high-throughput screening of gene products. *FEBS Lett.*, **514**, 102-105.

Sawasaki, T., Ogasawara, T., Morishita, R. & Endo, Y. (2002b) A cell-free protein synthesis system for high-throughput proteomics. *Proc. Natl. Acad. Sci. USA*, **99**, 14652-14657.

Sehr, P., Zumbach, K. & Pawlita, M. (2001) A generic capture ELISA for recombinant proteins fused to glutathione S-transferase: Validation for HPV serology. *J. immunol. Methods*, **253**, 153-162.

Soga, Y., Komori, H., Miyazaki, T., Arita, N., Terada, M., Kamada, K., Tanaka, Y., Fujino, T., Hiasa, Y., Matsuura, B., Onji, M. & Nose, M. (2009) Toll-like receptor 3 signaling induces chronic pancreatitis through the Fas/Fas ligand-mediated cytotoxicity. *Tohoku J. Exp. Med.*, **217**, 175-184.

Takahashi, S., Itoh, J., Nose, M., Ono, M., Yamamoto, T. & Kyogoku, M. (1993) Cloning and cDNA sequence analysis of nephritogenic monoclonal antibodies derived from an MRL/lpr lupus mouse. *Mol. Immunol.*, **30**, 177-182.

Takai, K., Sawasaki, T. & Endo, Y. (2010) Practical cell-free protein synthesis system using purified wheat embryos. *Nat. Protoc.*, **5**, 227-238.

Tan, E.M. (1989) Antinuclear antibodies: diagnostic markers for autoimmune diseases and probes for cell biology. *Adv Immunol.*, **44**, 93-151.

Theofilopoulos, A.N. & Dixon, F.J. (1985) Murine models of systemic lupus erythematosus. *Adv. Immunol.*, **37**, 269-390.

Theofilopoulos, A.N., Kofler, R., Singer, P.A. & Dixon, F.J. (1989) Molecular genetics of murine lupus models. *Adv. Immunol.*, **46**, 61-109.

Valdés Veliz, R., García, J., Reyes, B., Muñoz, L., Alvarez, T., Padilla, S., Abrahantes Mdel, C., Zubiaurrez, J., Agraz, A. & Marrero, A. (2003) A very sensitive enzyme-linked immunoabsorbent assay to Staphylococcal protein A in the presence of immunoglobulins. *Biochem. Biophys. Res. Commun.*, **303**, 863-867.

# Delivery of Na/I symporter gene into skeletal muscle by using nanobubbles and ultrasound: Visualization of gene expression by positron emission tomography

Yukiko Watanabe[1], Sachiko Horie[1], Yoshihito Funaki[2], Youhei Kikuchi[3], Hiromichi Yamazaki[2], Keizo Ishii[2,3], Shiro Mori[4], Georges Vassaux[5, 6], and Tetsuya Kodama[1]

[1]Graduate School of Biomedical Engineering, Tohoku University, Sendai, Japan.

[2]Cyclotron and Radioisotope Center, Tohoku University, Sendai, Japan.

[3]Graduate School of Engineering, Tohoku University, Sendai, Japan

[4]Tohoku University Hospital, Sendai, Japan.

[5]INSERM U948, Nantes, France.

[6]Institut des Maladies de l'Appareil Digestif, CHU Hôtel Dieu, Nantes, France.

Corresponding author:
Tetsuya Kodama, Ph.D., Professor
Molecular Delivery System Laboratory
Department of Biomedical Engineering
Graduate School of Biomedical Engineering, Tohoku University
2-1 Seiryo-machi, Aoba-ku, Sendai 980-8575, Japan
Phone & Fax: +81-22-717-7583
E-mail: kodama@bme.tohoku.ac.jp

**Running Title:** Gene delivery using US/NB & PET imaging

**Abstract**

**Subjects**: The development of non-viral gene delivery systems is essential in gene therapy, and the utilization of minimally-invasive imaging methodology can provide important clinical endpoints. In the present study, we present a new methodology for gene therapy: a delivery system by using nanobubbles (NB) and ultrasound (US) as a non-viral gene delivery method. We assessed whether the gene transfer allowed by this methodology is detectable by positron emission tomography (PET) as well as bioluminescence imaging. **Methods**: Two kinds of reported vectors (luciferase and human Na/I symporter (hNIS)) were transfected or cotransfected into the skeletal muscles of normal mice (BALB/c) by using the US/NB method. The kinetics of luciferase gene expression were analyzed *in vivo* by using bioluminescence imaging. At the peak of gene transfer, PET imaging of hNIS expression was performed using our developed Fine Structure Imaging PET scanner, following $^{124}I$ injection. The imaging data were confirmed using RT-PCR amplification, biodistribution, and a blocking study. The imaging potential of the two methodologies was evaluated in two mice models of human pathology (McH/lpr-RA1 mice showing vascular disease, and C57BL/10-mdx Jic mice showing muscular dystrophy). **Results**: Peak luciferase gene activity was observed in the skeletal muscle 4 d after transfection. On day 2 after hNIS and luciferase cotransfection, the expression of these genes was confirmed by RT-PCR on a

muscle biopsy. PET imaging of the hNIS gene, biodistribution, the blocking study, and autoradiography were carried out on day 4 after transfection, and it was indicated that hNIS expression was restricted to the site of plasmid administration (skeletal muscle). Similar localized PET imaging and $^{124}I$ accumulation were successfully obtained in the disease-model mice. **Conclusion**: The human NIS gene was delivered into the skeletal muscle of normal and disease model mice by the US/NB method, and gene expression was successfully visualized with PET. The combination of US/NB gene transfer and PET imaging may be applied to gene therapy clinical protocols.

**Key word**: PET; $^{124}I$; NIS gene; nanobubbles; ultrasound

## Introduction

Gene therapy approaches have been used in many different clinical contexts using a diverse range of pre-clinical models *(1, 2)*. Although viral vectors have been widely used in gene therapy, side effects such as carcinogenesis, hepatic toxicity, immunogenic, inflammation, and lower tissue specificity have been reported *(3, 4)*. In this context, the development of efficient non-viral methods of gene transfer is highly desirable and is the subject of intense investigation.

The combination of nanobubbles (NB) and ultrasound (US) has been proposed as

a strategy to deliver therapeutic molecules *(5)*, including plasmid DNA (*6, 7*). The principle is that when NBs are destroyed by US, the surrounding cells are exposed to mechanical impulsive forces generated by the collapse of either the NBs or the cavitation bubbles created by the collapse of the NBs. These forces induce a transient membrane permeability of cells, followed by the entry of exogenous molecules into the cells *(8)*. This mode of gene delivery has been proposed for different clinical applications including cancer gene therapy and vaccination strategies (*6, 7*)

In this context, molecular imaging could provide a minimally-invasive clinical end-point to monitor the efficacy of gene transfer. To evaluate the efficacy as well as the anatomical site of gene delivery, this methodology requires a reporter gene as well as a tracer molecule. Fluorescence and bioluminescence imaging methods have been widely used for the *in vivo* monitoring of gene expression in animal models *(9)*. These methods are convenient; however, their clinical application remains limited as signals generated in deep tissues cannot be detected. An alternative to these methods is the use of isotopic imaging (PET or SPECT imaging). The Na/I symporter (NIS) gene has been proposed as a valid reporter gene for isotopic imaging when it is associated with a relevant radiotracer. The NIS gene is an integral plasma membrane glycoprotein, endogenously expressed in the thyroid and stomach, and to a lower extent in the salivary gland, breast, and thymus. The NIS protein

uses the Na gradient in cells to concentrate iodide *(10)*. After the human NIS (hNIS) gene was cloned in 1996 *(11)*, we and others have proposed the use of NIS combined with $^{99m}$Tc or $Na^{123}I$ (for SPECT imaging) *(12)* or $Na^{124}I$ (for PET imaging) *(13, 14)* as reporter systems to visualize and monitor gene transfer in live subjects. These imaging devices have been recently validated in humans *(15)*.

Most current scintillator PET scanners are full width at half maximum (FWHM), providing a 1.3-mm reconstructed image resolution at the center of the field of view (FOV) and a 2-mm reconstructed image resolution within the central 5-cm diameter in all 3 dimensions *(16)*. This resolution is sufficient for imaging studies in rats. Recently, Ishii et al. developed a practical semiconductor animal PET with a CdTe detector ("Fine Structure Imaging PET": Fine-PET) *(17)*. The Fine-PET scanner achieves a spatial resolution of 0.8 mm FWHM within the central 20-mm diameter of the FOV and provides a high spatial resolution of less than 1 mm FWHM, which is applicable to studies in mice.

In the present study, we evaluated whether NIS gene expression mediated by US and NB could be detected by the Fine-PET in mice by using $^{124}I$ as radiotracer.

## Materials and Methods

### Plasmid DNA

Two types of plasmids were used: the luciferase reporter vector, pGL3 (pGL3-control, Promega, Madison, WI, USA), in which the luciferase expression is driven by the Simian virus 40 (SV40) promoter, and the human NIS (hNIS) vector, in which the expression of the hNIS gene is driven by the cytomegalovirus (CMV) promoter *(18)*. In both cases, the promoters are strong and allow ubiquitous expression of the transgene. The plasmids were purified with an EndoFree Plasmid Mega Kit (QIAGEN, Hilden, Germany), and prepared at a final concentration of 1 mg/mL.

**Nanobubbles**

Acoustic liposomes (ALs) were used as nanobubbles. One milliliter of a liposome suspension (lipid concentration: 1 mg/mL) was sonicated with a 20-kHz sonicator (Vibra-Cell™; Sonics & Materials Inc, Newtown, CT, USA.) in the presence of $C_3F_8$ in 7-mL sterilized vials. The bubble size distribution was determined using a laser diffraction particle size analyzer (particle range of 0.6 nm–7 μm. ELSZ-2; Otsuka Electronics Co. Ltd, Osaka, Japan). The peak diameter expressed in terms of the size distribution and the zeta potential of the ALs were 198 ± 30 nm ($n = 3$) and –4.1 ± 0.85 mV ($n = 3$), respectively.

**Ultrasound conditions and transfection methods**

A 1-MHz submersible US probe with a diameter of 30 mm (BFC Applications, Fujisawa, Japan) was used in the experiments. Signal generation and pressure measurements were as

previously described *(5), (6)*. After shaving the legs, the tibialis anterior (TA) muscle was immersed in water and exposed to ultrasound. The intensity was 3.0 W/cm$^2$; the duty cycle was 20%; the number of pulses was 200; the pulse repetition frequency (PRF) was 1000 Hz; and the exposure time was 60 s.

**Animal models**

Animal studies were performed in accordance with the ethical guidelines of Tohoku University. Three types of mice were used: 40 BALB/c; 5 McH/lpr-RA1 mice showing arthritis and vasculitis disease *(19)*; and 3 C57BL/10-mdx Jic mice showing muscular dystrophy. The mice were housed in the Animal Research Institute of Tohoku University Graduate School of Medicine under specific pathogen-free conditions, and had free access to food and water until the beginning of the experiments.

**Kinetics of gene expression induced by US and NBs**

Seven BALB/c mice (6 weeks old, weight 22–23 g) were used to investigate the kinetics of gene expression in the TA muscle. Two conditions were considered: pGL3 + US ($n = 3$) and pGL3 + US + NB ($n = 4$). A total volume of 30 μL comprising pGL3 (10 μL), with or without NB (15 μL), and saline (to reach 30 μL) was injected into the TA muscle. Mice were anesthetized with isoflurane (Forene; Abbott Scandinavia AB, Solna, Sweden) and subsequently injected intraperitoneally (i.p.) with luciferin (150 mg/kg body weight;

Promega). After 10 min, the mice were placed in the chamber of an *in vivo* real-time bioluminescence imaging system (IVIS Lumina; Xenogen, Alameda, CA, USA) with a CCD camera (sensitivity: 400–900 nm) and the images were captured for 40 s.

**Cotransfection of pGL3 and hNIS in the TA muscle**

In order to confirm that the hNIS gene was expressed in the TA muscle by the US/NB method, hNIS and pGL3 were cotransfected into the TA muscle. Mice that showed enhanced bioluminescence were selected as samples for an $^{124}I$ study. A solution containing hNIS (10 μL), pGL3 (5 μL), and NBs (15 μL) was injected into the TA muscle.

**RNA isolation and RT-PCR for luciferase and NIS**

Nine BALB/c mice (5 weeks old, weight 18–20 g) were used to measure luciferase and NIS gene expression in the TA muscle by RT-PCR. Three conditions were considered: saline alone ($n = 3$); pGL3 + US + NB ($n = 3$); and pGL3 + hNIS + US + NB ($n = 3$). Two days after cotransfection, the TA muscles were removed from the mice (5-weeks-old BALB/c) after monitoring the bioluminescence. The biopsies were frozen in liquid nitrogen and homogenized using a homogenizer (Ika, Staufen, Germany). Total RNA were extracted with an RNeasy Midi Kit (QIAGEN) and an RNase-Free DNase Set (QIAGEN) according to the manufacturer's protocol. Total RNA was reverse-transcribed using the RNA PCR Kit (AMV) (Takara Bio Inc., Tokyo, Japan) according to the manufacturer's protocol (1 μg of

total RNA was used). The cDNAs were then subjected to polymerase chain reaction (PCR) amplification by using a Peltier thermal cycler (PTC-200; MJ Research, Hercules, CA, USA). The PCR conditions were as follows: β-actin: 3 min at 94 °C, and 30 cycles of denaturation at 95 °C for 30 s, annealing at 54 °C for 30 s, and extension at 72 °C for 60 s, concluded by 5 min of extension at 72 °C; luciferase and hNIS: 3 min at 94 °C, and 35 cycles of denaturation at 95 °C for 30 s, annealing at 53 °C for 30 s, and extension at 72 °C for 60 s, concluded by a 5 min extension cycle at 72 °C. The specific primers are shown in Table 1. The PCR products were then separated on a 2 % agarose gel.

**Table 1. Primer sequences**

| Primers | Sequences (5' to 3') | Genomic position | Size (bp) | Accession No. |
|---|---|---|---|---|
| β-actin F | CGACATGGAGAAGATCTGGC | 319-338 | 739 | NM_007393 |
| β-actin R | TCTTCATGGTGCTAGGAGCC | 1039-1058 | | |
| Luc F | CCTCATAGAACTGCCTGCG | 910-928 | 689 | U47296 |
| Luc R | AGACTTCAGGCGGTCAACGAT | 1579-1599 | | |
| *hNIS F | GCTGAGGACTTCTTCACCGGGGGCCG | 477-501 | 581 | U66088 |
| *hNIS R | GTCAGGGTTAAAGTCCATGAGGTTG | 1034-1058 | | |

*The pair of degenerate primers was designed by Huang et al. *(20)*.

**Preparation of $Na^{124}I$**

$^{124}I$ was produced by the $^{124}Te(p, n)^{124}I$ process, by irradiation of a $^{124}TeO_2$ target with 14 MeV protons of a 4 μA beam current depending on the target production yield of $^{124}I$. Dry distillation apparatus of $^{124}I$ that was similar to the previous study (*21*) was slightly modified.

The radioiodine activity in the NaOH trap (0.5 mL; 0.1 M) was monitored by a NaI scintillation detector. The calculated isotopic compositions were $^{124}I = 98$ % and $^{123}I = 1$% 95 hours after the end of bombardment (EOB), because of the high isotopic enrichment of the tellurium-124 oxide used for the target preparation (*22, 23*).

**Biodistribution of $^{124}I$**

Fourteen BALB/c mice (6 weeks old, weight 18–27 g) were used to study the biodistribution of $^{124}I$. The TA muscle in the left leg of the mice was cotransfected with pGL3 and hNIS. The TA muscle in the right leg was injected with saline alone as a control. Four days after cotransfection, mice were injected intravenously (i.v.) with 370 kBq Na124I dissolved in 100 μL PBS (pH in the physiological range) and sacrificed after 30 (thyroid: n = 1, the other tissues: n = 4), 60 (n = 6), and 180 (thyroid: n = 3, the other tissues: n = 4) minutes. The organs and tissues were quickly removed. Each sample was washed with saline solution and weighed. The radioactivity of each sample was measured by a γ-counter (AccuFLEX γ7000; ALOKA Co. Ltd., Mitaka, Japan) in the range of 400-700keV. The radioactivity of organs and tissues was expressed as the percentage of the injected dose per gram (%ID/g).

**Blocking study in the TA muscle**

Four BALB/c mice (6 weeks old, weight 21–25 g) were used for a blocking study in the TA muscle. All TA muscles were cotransfected with pGL3 and hNIS. Three days after